

# The influence of brittle failure and its impact on face stability in high-stress tunnelling conditions

Joel Chiwara

*University of Leeds, Leeds, United Kingdom*

Ioannis Vazaios

*Ove Arup & Partners Ltd, London, United Kingdom*

Chrysothemis Paraskevopoulou (corresponding author; c.paraskevopoulou@leeds.ac.uk)

*University of Leeds, Leeds, United Kingdom*

**ABSTRACT:** In deep hard rock environments under high-stress conditions, rockmasses behave in a brittle manner resulting in spalling and strain bursting. This paper examines the occurrence of brittle failure and its impact on face stability. Generalised Hoek-Brown failure criterion modified after the Damage Initiation and Spalling Limit (DISL) approach is adopted in 2D and 3D numerical models to capture the mechanical response of brittle rocks in underground excavations. Unsupported circular tunnel models are used to investigate brittle failure at the tunnel face. Excavation induced stress and deformation results show that under anisotropic in-situ stress conditions, models become unstable, and relaxation rapidly increases within 3 m behind the tunnel face, while within a distance of 0.85 times the tunnel radius, the tunnel relaxes 85% to 95%. This demonstrates the rapid loss of confinement in hard rock masses within the face vicinity which yields instabilities in the tunnel.

*Keywords: brittle failure, high-stress, tunnel face stability, strain bursting, hard rock tunnelling, deep mining*

## 1 INTRODUCTION

There has been significant growth in underground development in the last decades due to increased demand in infrastructure, energy storage, mining and resource extraction and the need for safer hazardous waste disposal facilities. Consequently, this has resulted in underground structures covering large areas and depths exceeding several kilometers and excavated in high-stress rock mass environments. Rockmass materials under such high-stress conditions tend to behave in a brittle manner during excavation (Diederichs 2007). Brittle failure manifesting as spalling and strain bursting has been extensively examined by several researchers and identified as a significant subject in deep tunnelling (Kaiser et al. 1996). Underground excavations alter the field stress state with the induced stress redistributions resulting in fracturing, disturbance and deformations around the openings. Hence, it is critical to understand the excavation response and related brittle failure manifesting, such as spalling, which influences the support requirements, excavation advance rates and other design and construction aspects. Various researchers (Kaiser et al. 1996, Diederichs 2007) have contributed in developing mechanistic interpretations, empirical methods and semi-empirical approaches of predicting excavation-induced damage in massive rock masses. However, recent years have seen a growing interest in research and application of numerical modelling in predicting rockmass behaviour under such conditions. In this research the Finite Element Method (FEM) and the Damage Initiation and Spalling limit (DISL) constitutive approach introduced by Diederichs (2007) are used to investigate the excavation response of deep underground openings in hard rock masses.

## 2 BRITTLE FRACTURING IN DEEP EXCAVATIONS

Spalling and strain bursting are the dominant failure mechanisms in deep underground openings in hard, massive rock masses and have been extensively studied by several researchers (Diederichs 2007, Vazaios et al. 2019, Aujmaya et al. 2023). Spalling is a failure mode in which extensile fractures develop near excavation boundaries under high compressive loading. In contrast, strain bursting is a violent ejection of excavation wall rocks under high compressive stress that occurs in brittle and dilatational process failure.

Spalling is commonly observed around excavation openings in high compressive stress and low confinement conditions and is controlled by the internal tensile strength of the material. Lee et al. (2004) established that a criterion for spalling potential could be developed based on the Unconfined Compressive Strength (UCS) to Tensile strength (T) ratio. UCS accumulates strain energy, increasing the potential for strain bursting, whereas a lower UCS /T ratio suggests a higher spalling potential. Notably, spalling can be violent or non-violent. Wiid (1970) suggested that spalling can be a time-dependent process where the strain boundary conditions are static, despite its brittle nature. To capture the rock mass behaviour under such conditions in the continuum numerical modelling analysis, the DISL empirical constitutive model based on the Hoek-Brown criterion parameters was developed by Diederichs (2007), assuming an instantaneous loss of cohesion and mobilization of friction once fracturing starts occurring (Figure 1).

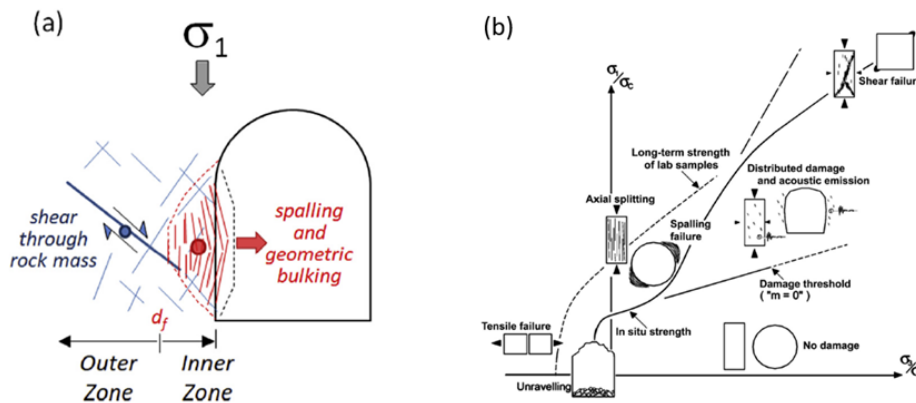


Figure 1. a. Underground openings dominated by spalling under low confinement conditions transitioning to shear based failure under higher confinement (after Gao et al. 2019) b. Composite strength envelope as based on DISL (Diederichs 2007).

## 3 NUMERICAL MODEL SETUP

For the purposes of this paper, numerical modelling is undertaken to simulate the brittle behaviour of rock masses to examine the excavation face response, and the Hoek-Brown failure criterion is modified as per the DISL model and applied in Rocscience RS2 and RS3 FEM software.

### 3.1 Geometrical, Mesh and Boundary Conditions Setup

A circular tunnel geometry is adopted to investigate the influence of brittle failure at the excavation face. The excavation is designed to be 7 m in diameter, as shown in Figure 2. In the 2D models, the external boundary is selected to be square-shaped and 80 m in length, thus approximately eleven times the excavation diameter to minimize potential boundary effects during the analysis. For the 3D models, a cube-shaped external box 80 m in length in each dimension is modelled. In both 2D and 3D models, the outer boundaries are restrained in all directions, and all models are examined to confirm the absence of boundary influence on the depth of plastic yielding. The mesh comprises of six-node triangular elements in the 2D models and four-node tetrahedral elements in the 3D models. Pins are assigned on all sides to simulate the far-field conditions under the assumption of a deep tunnel.

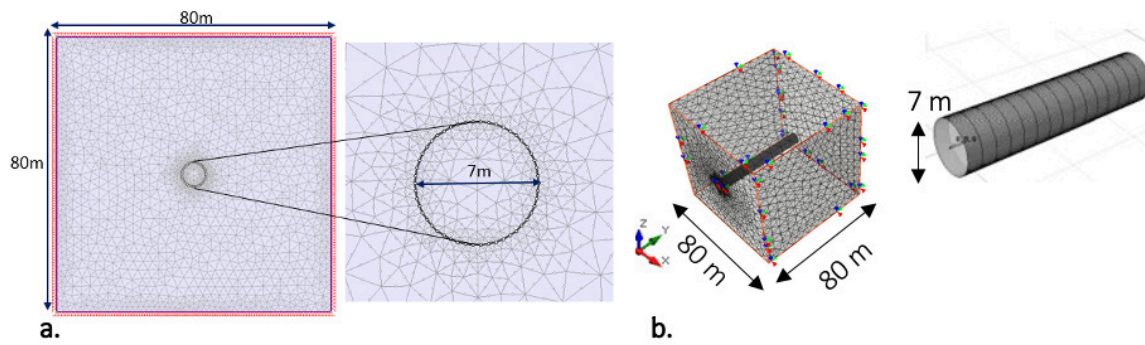


Figure 2. Tunnel model configuration created in a. 2D (RS2) and b. 3D (RS3) for a circular tunnel.

### 3.2 Field Stresses

Four stress scenarios are used in the undertaken numerical modelling to investigate the influence of stress magnitudes on brittle failure. In each scenario, the model assumes a constant vertical stress of 13.25 MPa, calculated from an assumed overburden depth of 500 m and a constant rock mass density of 2700 kg/m<sup>3</sup>. Another primary assumption is that the tunnels are very deep with uniform constant stress, so the effect of gravitational forces and gravity-induced stress gradients is negligible. Uniform lateral pressure coefficients of  $K=2, 3$  and  $4$  are assumed in the four cases. It should be noted only results from the  $K=4$  are shown for the purposes of this paper.

### 3.3 Excavation Sequence

Tunnelling is a process with 3D effects; therefore, to capture the three-dimensional (3D) impact of the tunnel advance in 2D, an internal pressure ( $p_0$ ) equal to the geostatic stress was initially applied as a distributed load around the tunnel boundary. Prior to any excavation, the first stage is used to establish the in-situ stresses and ensure static equilibrium at the geostatic stage of the analysis. Afterwards, the excavation is simulated in stages in which for the 2D models,  $p_0$  was progressively reduced in each excavation step until complete relaxation was achieved. For the 3D models, the tunnels are modelled at 60 m length, a distance sufficient to eliminate potential boundary effects during the analysis. Tunnel excavation is simulated in 3 m stages, which is a typical advance in drill and blast tunnels in deep massive hard rock environments (Paraskevopoulou & Diederichs, 2018).

### 3.4 Material Properties

The intact rock mechanical properties for the granitic rock were obtained from Mahabadi et al. (2012), whilst gneissic rock properties are obtained from Berčáková et al. (2020) and are shown in Table 1.

Table 1. Input parameters for all FEM numerical models.

	Parameter	Granite	Gneiss
FEM - DISL	UCS (MPa)	138.5	95.38
	Young's modulus (E) (GPa)	52	21.63
	Poisson's ratio ( $\nu$ )	0.4	0.07
	Peak	0.25	0.25
	Parameter $s$	0,033	0.033
	Parameter $m_b$	1	1
	Residual	0.75	0.75
	Parameter $s$	0.001	0.001
	Parameter $m_b$	7	7

The major assumption made for the undertaken simulations is that the material behaves according to the DISL model and the rockmass is massive with no fractures. Furthermore, the tensile strength values are automatically assigned by the software. However, in the software the Hoek-Brown tensile strength is typically overestimated, which introduces a limitation in these models.

#### 4 NUMERICAL ANALYSIS AND RESULTS

Following the undertaken 2D and 3D numerical modelling by adopting different geological and stress conditions, the impact of brittle fracturing on the excavation face stability is investigated by interrogating stress paths and face extrusion, as shown in the sections below.

##### 4.1 2D and 3D Models

To assess when yielding and fracturing initiates at the tunnel boundary (crown), initially, the major and minor principal stresses from the conducted 2D analyses are examined. The principal stress paths are presented in Figure 3.

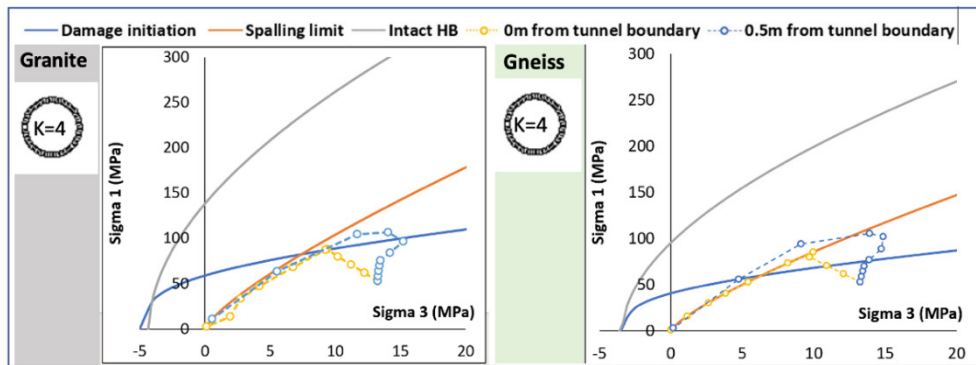


Figure 3. For a K=4 stress ratio, circular excavation 2D DISL models stress paths at tunnel boundary (crown) for Granite and Gneiss. The arrow shows the direction of the stress path, and the red dot indicates the initial geostatic stress.

Stresses are monitored at various stages representing a 10% reduction per excavation stage from the initial stresses ( $p_0$ ), which are then plotted against the DISL strength envelopes. Regarding brittle behaviour, the stress changes are scrutinised at the tunnel face as the tunnel advances and approaches the face under examination by extracting major and minor principal stresses. The respective stress paths are shown in Figure 4.

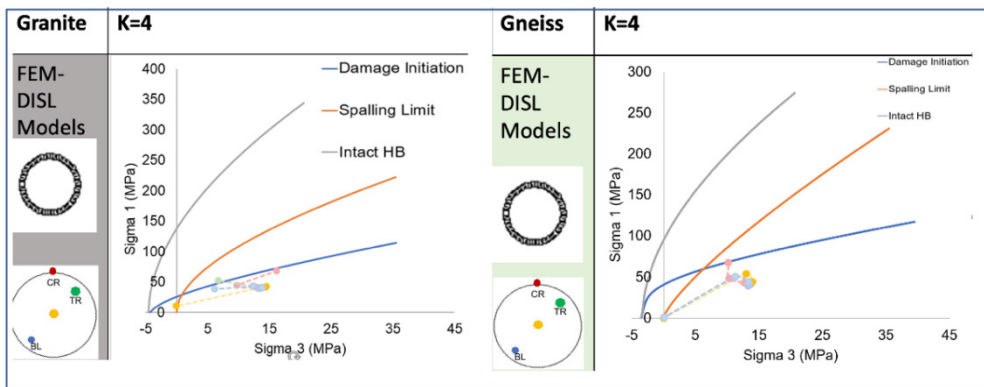


Figure 4. Circular tunnels for K=4 stress paths at four points on the tunnel face for Granite and Gneiss.

#### 4.2 2D and 3D Relaxation Correlation & Face Extrusion

As the tunnel advances, confinement decreases, resulting in stress-induced deformations. Face extrusion is interrogated to understand the amount of induced relaxation as the tunnel advances. Stress results from the 2D and 3D models are compared against each other to allow for the correlation between the two modelling approaches. The stress relaxation correlations are shown in Figure 5. Moreover, the 2D plain strain assumption fails to capture the extrusion of the tunnel face, thus necessitating 3D modelling to assess extrusion at the tunnel face.

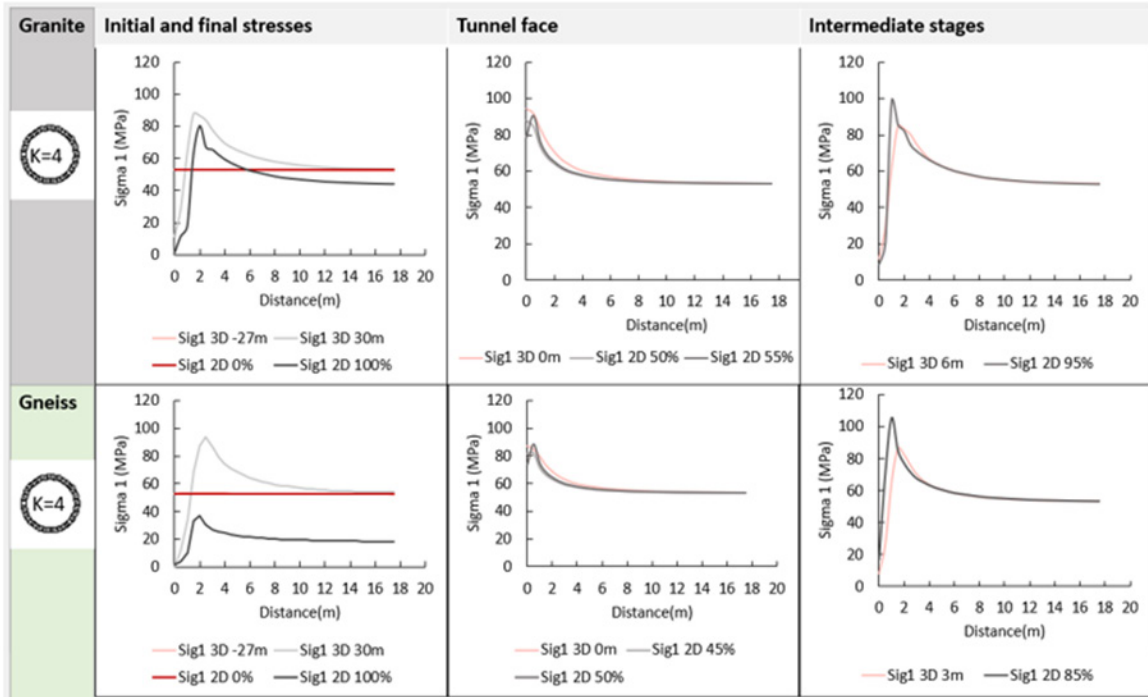


Figure 4. Correlation of 2D stress relaxations and 3D models' distance from excavation face for Circular excavations at K=4. Correlations are conducted at initial geostatic stresses, final excavation, tunnel face and intermediate points along the tunnel length.

The extrusion deformation is examined from the 3D FEM-DISL models to assess the face influence on the stability of brittle rockmasses. The results are as shown in Figure 5.

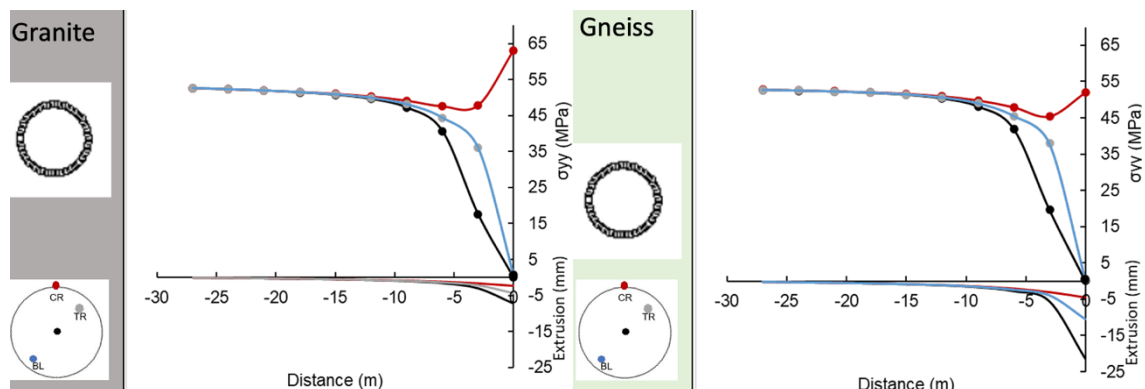


Figure 5. Circular K=4 models variation of extrusion (mm) and  $\sigma_{yy}$  with distance ahead of the tunnel face at crown, center, bottom left and top right.

## 5 DISCUSSION AND CONCLUSIONS

Numerical modelling using the FEM method coupled with the DISL constitutive approach captures the brittle behaviour of hard rockmasses in deep tunnels. A comparison of 2D and 3D major principal stresses shows a good correlation which proves the consistency of 2D and 3D models' results and a reasonable degree of confidence in the use of models to predict the brittle response of the tunnel face. The stress relaxation in 2D models is correlated to the distance from the tunnel face in 3D models to examine the amount of relaxation that the tunnel face experiences. Results demonstrate that as soon as the tunnel advances ahead of the face under examination, relaxation in the tunnel behind the face is rapid. At 3 m from the tunnel face, relaxation ranges from 85% to 90%. Brittle failure at the tunnel crown is characterised from 2D results stress paths plotted against the DISL strength envelopes. For a stress ratio of  $K=4$ , the crown is mainly characterised by spalling and slabbing. The intensity of the spalling increases with an increase in the stress ratio  $K$ . The tunnel face undergoes extrusion which ranges between 0 and 25 mm for the given geological conditions. Consistent in all results, the centre exhibits the highest extrusion, followed by the bottom right and top left monitoring points. This is because the tunnel centre experiences relatively lower confinement from the tunnel boundary, unlike the top right and bottom left points that are closer to the crown and floor, respectively. The results' trend shows an increase in extrusion with an increase in the stress ratio  $K$ . Finally, there is high variability in extrusion magnitudes depending on different geometries and geological environments. Gneiss excavations show at least twice as much extrusion as compared to the ones in granite for the examined materials.

## REFERENCES

- Aujmaya, L., Vazaios, I., and Paraskevopoulou, C., 2023. Assessing the tunnel stability in brittle rocks based on strain bursting assessment. In: Eurock 2022 - Rock and Fracture Mechanics in Rock Engineering and Mining IOP Publishing IOP Conf. Series: Earth and Environmental Science 1124 (2023) 012089 doi:10.1088/1755-1315/1124/1/012089
- Berčáková, A., Melichar, R. and Souček, K. 2020. Mechanical Properties and Failure Patterns of Migmatized Gneiss with Metamorphic Foliation Under UCS Test. *Rock Mechanics and Rock Engineering*. **53**(4), pp.2007–2013.
- Diederichs, M.S. 2007. The 2003 Canadian geotechnical colloquium: Mechanistic interpretation and practical application of damage and spalling prediction criteria for deep tunnelling. *Canadian Geotechnical Journal*. **44**(9), pp.1082–1116.
- Gao, F., Kaiser, P.K., Stead, D., Eberhardt, E. and Elmo, D. 2019a. Strainburst phenomena and numerical simulation of self-initiated brittle rock failure. *International Journal of Rock Mechanics and Mining Sciences*. 116(July 2018), pp.52–63.
- Kaiser, P. K., McCreath, D. R. & Tannant, D. D., 1996. Canadian Rockburst Support Handbook. In: Canadian Rockburst Research Program, Vol II, Book I . Ontario: Canadian Mining Industry Research Organization, p. 343.
- Lee, S. M., Park, B. S. & Lee, S. W., 2004. Analysis of Rockbursts that have occurred in a Waterway Tunnel in Korea. *International Journal of Rock Mechanics and Mining Sciences*, Volume 41, pp. 911-916.
- Mahabadi, O.K., Randall, N.X., Zong, Z. and Grasselli, G. 2012. A novel approach for micro-scale characterization and modeling of geomaterials incorporating actual material heterogeneity. *Geophysical Research Letters*. 39(1), pp.1–7.
- Paraskevopoulou, C., Diederichs, M., 2018. Analysis of time-dependent deformation in tunnels using the Convergence-Confinement Method. *Tunnelling and Underground Space Technology Journal*, 71(2018), 62-80, 19 pages. <http://dx.doi.org/10.1016/j.tust.2017.07.001>
- Vazaios, I., Diederichs, M.S. and Vlachopoulos, N. 2019. Assessment of strain bursting in deep tunnelling by using the finite-discrete element method. *Journal of Rock Mechanics and Geotechnical Engineering*. 11(1), pp.12–37.
- Wiid, B.L. 1970. The influence of moisture on the pre-rupture fracturing of two rock types. In *Proceedings of the 2nd Congress of ISRM.*, Belgrade. Vol.2, No. 3-4, pp. 239-245